Atmos. Chem. Phys. Discuss., 10, 26641–26676, 2010
www.atmos-chem-phys-discuss.net/10/26641/2010/
doi:10.5194/acpd-10-26641-2010

Atmospheric Chemistry and Physics Discussions

Characterization of individual aerosol particles collected during a haze episode in Incheon, Korea using the quantitative ED-EPMA technique

H. Geng[1,2], J. Ryu[1], S. Maskey[1], H.-J. Jung[1], and C.-U. Ro[1]

[1]Department of Chemistry, Inha University, Incheon, 402-751, Korea
[2]Research Center of Environmental Science and Engineering, Shanxi University, Taiyuan, 030006, China

Received: 3 September 2010 – Accepted: 30 October 2010 – Published: 8 November 2010

Correspondence to: C.-U. Ro (curo@inha.ac.kr)

Published by Copernicus Publications on behalf of the European Geosciences Union.

Abstract

Haze is an atmospheric phenomenon that leads to low visibility, and is mostly due to elevated levels of fine particulate matter. It can have effects on cloud formation, public health, agriculture, and even the global climate. Although urban haze has been increasing in occurrence over the past several years over the Seoul-Incheon metropolis, Korea, studies of the morphology and chemical composition of ambient aerosol particles by single-particle analysis during haze episodes have rarely been conducted. Herein, a quantitative energy-dispersive electron probe microanalysis (ED-EPMA), called low-Z particle EPMA, was used to analyze individual aerosol particles collected in Incheon, Korea on 13–18 October 2008 (a typical haze episode occurred from 15 to 18 October). Overall, 3600 particles in 12 aerosol samples collected on haze and non-haze days were measured by low-Z particle EPMA. Based on quantitative X-ray analysis, together with secondary electron images of individual particles, we successfully identified the aerosol particle types as follows: elemental carbon (EC), organic carbon (OC), $(NH_4)_2SO_4/NH_4HSO_4$-containing, genuine (fresh) and reacted (aged) sea-salt, mineral dust (such as aluminosilicate, SiO_2, $CaCO_3/CaMg(CO_3)_2$, etc.), and K-containing, Fe-rich, and fly ash particles. By analyzing the relative abundances of different particle types, it was concluded that (a) on non-haze days, reacted sea-salts and reacted mineral dust particles were abundant in both the $PM_{2.5-10}$ and $PM_{1.0-2.5}$ fractions (with relative abundances of 65.0% and 57.7%, respectively); whereas on haze days, the relative abundances of OC and $(NH_4)_2SO_4/NH_4HSO_4$-containing particles were significantly elevated, indicating that organic matter and secondary aerosols were abundant in the atmosphere when haze occurred. (b) in $PM_{2.5-10}$ fractions, sea-salt and mineral dust particles reacted with NO_x/HNO_3 significantly outnumbered those reacted with SO_2/H_2SO_4, no matter whether they were collected on haze or non-haze days; but in $PM_{1.0-2.5}$ fractions on non-haze days, the nitrate-containing reacted particles significantly outnumbered the sulfate-containing ones, whereas it was the reverse on haze days, implying that on haze days there were special sources or formation mechanisms

ACPD

10, 26641–26676, 2010

for the reacted fine aerosol particles (aerodynamic diameter<2.5 µm). It is hypothesized that motor vehicles, biomass burning from the areas surrounding Incheon, and haze transported from Eastern China are the major contributors to urban haze formation in Incheon under stagnant meteorological conditions such as low wind speed, high relative humidity, etc.

1 Introduction

Urban haze, an atmospheric phenomenon that leads to low visibility, has increased in occurrence over the last several years over the Seoul-Incheon metropolis and other cities in Korea, because of continuous economic growth and the increase of consumption of fossil fuels (Lee et al., 2006; Chun and Lim, 2004; Kim et al., 2008a). The occurrence of haze is closely related to meteorological conditions and air pollution (Keywood et al., 2003). Specifically, the formation of haze is favored by stagnant weather conditions and high emissions of air pollutants (Sun et al., 2006). For instance, under a temperature inversion, airborne smog, organic compounds, and particulate matter often fail to diffuse, persisting in the air over the city and thus inducing haze (Viezee and Oblanas, 1969). In general, urban haze is related to a high level of airborne particles resulting from anthropogenic emission (through industrial and other human activities) and from gas-to-particle conversion (Watson, 2002; Kim et al., 2008a). In turn, haze alters the composition of airborne aerosols through aqueous phase reactions (Sun et al., 2006), having significant effects on visibility, cloud formation, public health, and even the global climate (Davis et al., 2010; Yadav et al., 2003; Menon et al., 2002; Lee and Sequeira, 2001).

During urban haze episodes, water-soluble inorganic ions (such as NO_3^-, SO_4^{2-}, and NH_4^+) and carbonaceous species in $PM_{2.5}$ are considered important contributors to visibility impairment (Kang et al., 2004; Jacobson, 2001). It has been reported that in fine particle mass loading on haze days, ammonium sulfate and organic carbon are dominant (Kim et al., 2008a; Brown et al., 2002); on the other hand, haze decline has

ACPD
10, 26641–26676, 2010

been shown to be consistent with reduction of $PM_{2.5}$ and sulfur emissions (Schichtel et al., 2001).

In Korea, the annual number of low-visibility days has significantly increased due to the occurrence of fog, mist, and haze (caused largely by increasing emission of anthropogenic air pollutants such as fine particles, NO_x, SO_2, and organic compounds), especially in urban areas (Kim et al., 2008a; Chung et al., 1999). Several studies on the spatial variation of visibility and climatic characteristics of haze episodes in the Seoul-Incheon metropolis have been carried out (Chun and Lim, 2004; Kang et al., 2004). However, the chemical characteristics and morphologies of individual airborne particles on haze days in this region have rarely been investigated. In fact, such studies are needed because (1) the detailed information on homogeneous/heterogeneous aerosol particles' microphysical and chemical properties can deepen our understanding of the sources, reactivity, transport, and removal of airborne particles (Geng et al., 2009a, b, 2010); (2) it can reflect the influence of continental outflow events on aerosol compositions, since Incheon, located on the west coast of Korea, is one of the Korean cities nearest to China, being frequently impacted by air masses originating from Mongolia and China.

In the present work, a quantitative energy-dispersive electron probe X-ray microanalysis (ED-EPMA) method called low-*Z* particle EPMA, was used to characterize ambient aerosol particles collected in Incheon on haze and non-haze days. This single-particle analytical technique, which is based on scanning electron microscopy (SEM) coupled with an ultra-thin window energy-dispersive X-ray spectrometer (EDX), can not only simultaneously detect the morphology and constituent elements of a single particle, but also provide transformation information on many environmentally-important particles of micrometer size, such as nitrates, sulfates, oxides, or mixtures, including carbon matrices (Ro et al., 2006; Choel et al., 2005).

The objective of the present study was to identify the ambient aerosol particle types, and compare their relative abundance distribution during a typical haze episode (occurring on 15–18 October, 2008) with that on non-haze days by using low-*Z* particle

ACPD
10, 26641–26676, 2010

EPMA, and to investigate possible contributing factors to haze formation in Incheon, Korea.

2 Materials and methods

2.1 Sampling

Incheon, located on the coast of the Yellow Sea, is densely populated, with 2.7 million people in an area of 958 km^2. It is the third largest metropolis, and one of the most important transport hubs, in Korea. A part of Incheon borders the capital city, and the Seoul-Incheon subway systems are linked, so Incheon is considered a part of the greater Seoul metropolitan area. Incheon has many different local emission sources, including seven industrial complexes, two seaports with ten wharfs, and one international airport. The sampling site, regarded as being susceptible to various urban source processes, was located on the roof of a five-story building (about 20 m above the ground) of Inha University, Incheon (latitude 37.45° N, longitude 126.73° E, see Fig. 1). Aerosol particles were collected on Al foils by using a three-stage cascade impactor (Dekati PM-10 sampler, Dekati Ltd.). At a flow rate of 10 L min^{-1}, the aerodynamic cut-off diameters for stages 1–3 were >10, 2.5–10, and 1.0–2.5 µm, respectively. Particles collected on stages 2 and 3 were analyzed for each sample set. Overall, 12 sets of samples were obtained in the morning and evening on 13–18 October 2008. During the sampling, the collecting duration for each stage sample was controlled so that particles were collected without overloading. Sampling dates, temperature (T), relative humidity (RH), and average wind speed during the sampling are given in Table 1.

The 72-h backward air-mass trajectories at a receptor height of 40 m above sea level were produced using the HYbrid Single-Particle Lagrangian Integrated Trajectory (HYSPLIT4) model available at the NOAA Air Resources Laboratory's web server (http://www.arl.noaa.gov/ready/hysplit4.html) (Fig. 2).

ACPD
10, 26641–26676, 2010

2.2 Data measurement and analysis

A swatch of Al foil containing the sample particles was cut and observed. The measurements were carried out on a JEOL JSM-6390 SEM equipped with an Oxford Link SATW ultra-thin window EDX detector. The resolution of the detector was 133 eV for a Mn-Kα X-ray. X-ray spectra were recorded under the control of INCA software (Oxford), with an accelerating voltage of 10 kV and beam current of 0.5 nA. The size, secondary electron image (SEI), chemical compositions, and mixing state of 150 individual particles for each stage sample (3600 particles overall for 24 stage samples) were investigated manually. The net characteristic X-ray intensities of chemical elements were evaluated by a nonlinear least-squares fitting using the AXIL program (Vekemans et al., 1994). A Monte Carlo simulation with successive approximation was used for quantification (Ro et al., 2003). The elemental quantification procedure provided results with an accuracy of within 12% relative deviations between the calculated and nominal elemental concentrations for the standard particles (Ro et al., 2000, 2001). The "expert system" program, which can rapidly and reliably perform chemical speciation, was used to determine the formula concentrations and particle group distributions (Ro et al., 2004).

The basic classification rules are here briefly summarized. Firstly, a particle was regarded as being composed of just one chemical species if this species constituted at least 90% in atomic fraction. Secondly, chemical species were specified for particles internally mixed with two or more chemical species. Thirdly, elements with less than 1.0 at.% (atomic percent concentration) were neglected, since elements at trace levels cannot be reliably investigated using ED-EPMA.

ACPD
10, 26641–26676, 2010

3 Results and discussion

3.1 Particle types

In this work, analyzed particles were classified based on their X-ray spectral and SEI data. Particle types that were abundantly observed in the samples were carbonaceous, $(NH_4)_2SO_4/NH_4HSO_4$-containing, sea-salt, mineral dust, K-containing, Fe-rich, and fly ash particles. The characteristics of each particle type are described below.

3.1.1 Carbonaceous particles

Carbonaceous aerosol particles are one of the most important components of urban aerosols (especially in fine fractions), which can account for up to 40% of $PM_{2.5}$ mass in an urban atmosphere (Feng et al., 2009). Generally, they are differentiated into two groups: elemental carbon (EC) and organic carbon (OC) (Arimoto et al., 2006; Li and Bai, 2009). With respect to their chemical properties, there are great, but not absolutely distinct, differences between EC and OC (Arimoto et al., 2006). For both EC and OC particles, the sum of the C and O content (sometimes including N) is more than 90 at.% (Geng et al., 2010). EC particles are also termed "carbon-rich particles", because the concentration of C is much larger (generally more than 3 times) than that of O, and almost no other element is present in them (Geng et al., 2009a). Herein, three types of EC particles were identified based on the morphologies and X-ray spectral data. The first type is soot aggregates, which appear in a fractal-like chain structure (e.g., particles #16, #68, and #82 in Fig. 3), even after being surrounded by organic matter (Adachi et al., 2010); the second type is tar balls, which appear as separate spherules (e.g. , particles #26, #39 and #129 in Fig. 3), being largely produced from smoldering combustion and existing in abundance in polluted continental air masses (Chakrabarty et al., 2010); and the third type is chars or coal dust particles, which have an irregular-shaped structure (e.g., particle #56 in Fig. 3). The X-ray spectra of the three types are similar (Fig. 4), although the morphologies of tar balls and chars are quite different from that of soot aggregates.

ACPD
10, 26641–26676, 2010

OC accounts for a large portion of submicron atmospheric aerosol particles, and OC particles can account for 30%–90% of the total urban particle mass (Takahama et al., 2007). Organic aerosol particles can be either emitted directly from primary sources such as biogenic particles and generated in meat cooking, cigarette smoking, and various combustion processes, or formed as secondary aerosol products (a large amount of organic aerosol mass in urban areas is of secondary organic aerosol (SOA)) (Moffet et al., 2010). In the present study, two clearly different types of OC particles were observed. One of these is perhaps primary or water-insoluble secondary organic particles, which look bright and angular on their SEIs, and have high levels of C and O or C, O, and S; e.g., #14, #38, #42, #49, #59-#61, #63-#65, #69, #71-#74, #79, #80, #83, #84, #86, and #111 in Fig. 3. The other type is liquid droplet particles, which are rich in C, O, and S (occasionally C and O) and represented as CO-rich or COS-rich droplets (Fig. 5). They appear dark and round on SEI, probably containing water-soluble secondary organic aerosol (WSOA) or mixing with a small amount of $(NH_4)_2SO_4/NH_4HSO_4$. These droplet particles are small in diameter, frequently encountered in $PM_{1.0-2.5}$ fractions (e.g., particles #19, #21, #25, #29, #30, #32, #33, #34, #106-#123, 125-#128, #131, and #133 in Fig. 3), and can be comprised of oxidation of volatile organic compounds, humic substances, or "humic-like substances (HULIS)", and incomplete combustion of fossil fuels and biomass (Aiken et al., 2009).

3.1.2 $(NH_4)_2SO_4/NH_4HSO_4$-containing particles

Ambient sulfate/bisulfate/H_2SO_4 is often neutralized by ammonia (mainly from animal waste, fertilizer application, soil and industrial emissions, and direct emissions from vegetation and oceans). The most common product is ammonium sulfate, but if ammonia is scarce, sulfate remains in its more acidic forms such as NH_4HSO_4 or H_2SO_4 (Millstein et al., 2008). The SEIs of $(NH_4)_2SO_4/NH_4HSO_4$ particles (e.g., particles #124, #130, and #132 in Fig. 3) show holes in them, possibly due to electron beam damage, and their EDX spectra show peaks of C, N, O, and S, or just C, O, and S (more than 95% atomic fractions of (C+N+O+S) or (C+O+S) were detected

ACPD
10, 26641–26676, 2010

for these particles). Also, N signals sometimes fail to be observed, possibly due to beam damage on the $(NH_4)_2SO_4/NH_4HSO_4$-containing particles. Water-soluble organic (or carbon-rich) aerosols are often internally mixed with $(NH_4)_2SO_4/NH_4HSO_4$ particles, especially in urban atmosphere (Johnson et al., 2005; Adachi and Buseck, 2008). Moffet and Prather (2009) found that in areas of high pollution and its surroundings, much of the soot is embedded within OC, together with materials such as $(NH_4)_2SO_4/NH_4HSO_4$. Adachi et al. (2010) suggested that organic material and/or $(NH_4)_2SO_4$ initially condensed onto the surface of soot particles and then subsequently filled the spaces between their branches. Therefore, it is sometimes difficult to clearly distinguish $(NH_4)_2SO_4/NH_4HSO_4$-containing particles from organic droplet particles rich in C, O, and S.

3.1.3 Sea-salt aerosols

There exist a large number of sea-salt aerosols (SSA) on marine boundary layers and in coastal regions (Athanasopoulou et al., 2008; Oum et al., 1998). Genuine (or fresh) and reacted (or aged) sea-salt aerosol particles could be clearly identified by low-Z particle EPMA. For genuine sea-salt particles (e.g. particle #2 in Fig. 3), Na and Cl signals are predominant in their X-ray spectra, with an atomic concentration ratio of [Na]:[Cl] $\approx$ 1:1. Minor C and O X-ray peaks were often concomitant, suggesting that organic matters were adsorbed on them and/or an NaOH shell, an alkaline hygroscopic coating around the NaCl, was present (Laskin et al., 2003). For the reacted sea-salts, $NaNO_3$ and/or Na_2SO_4, which were sometimes mixed with $NaCl/MgCl_2$, were observed, indicating that the reacted (or aged) sea-salts were produced in the atmosphere when genuine sea-salts reacted with nitrogen and sulfur oxides (usually resulting in chlorine loss). It has also been suggested that SSA often acted as a sink for anthropogenic gases such as NO_x and SO_2 (Laskin et al., 2002; Hoffman et al., 2004).

Herein, based on their SEI and X-ray spectral data, the reacted sea-salts were classified into three types. The first was for those containing nitrates such as Na(Cl, NO_3)

ACPD
10, 26641–26676, 2010

and (Na, Mg)(Cl, NO_3), which are the reaction products of genuine sea-salts and NO_x/HNO_3 (e.g., particles #6, #43, and #100 in Fig. 3); the second was for those containing sulfates, such as Na_2SO_4 and (Na, Mg)SO_4, which result from the reaction of genuine sea-salts with SO_2 or H_2SO_4 (e.g., particles #67 and #98 in Fig. 3); and the third was for those containing both nitrates and sulfates (e.g., particles #44 and #53 in Fig. 3). The reacted sea-salts were sometimes mixed with mineral dust particles. Their typical X-ray spectra have been given elsewhere (Geng et al., 2009a, b, 2010). These particles were classified into the "reacted sea-salt & mixture" group (e.g., particles #18 and #91 in Fig. 3).

3.1.4 Mineral dust particles

Mineral dust particles appear irregular and bright on their SEIs (Fig. 3). The typical genuine mineral dust particles include aluminosilicate (AlSi-containing; e.g., particles #8, #11, #22, #40, #51, #54, #55, #57, #66, #87, #93, and #94 in Fig. 3), quartz (SiO_2, e.g., particles #46 and #58 in Fig. 3), calcite ($CaCO_3$)/dolomite ($CaMg(CO_3)_2$) (e.g., particles #37, #50, and #62 in Fig. 3), and gypsum ($CaSO_4{\cdot}2H_2O$). The obtained atomic concentration ratios for SiO_2 and $CaCO_3$ are close to stoichiometric, i.e., [Si]:[O] $\approx$ 1:2, and [Ca]:[C]:[O] $\approx$ 1:1:3. But for aluminosilicate particles, with strong X-ray peaks of Al, Si, and O, the contents of minor elements such as Na^+, K^+, Ca^{2+}, Mg^{2+}, and Fe^{2+} in them are liable to vary, since aluminosilicates have a wide variety of species and crystalline structures such as feldspar, mica, kaoline, zeolites, etc. (Jung et al., 2010).

Reacted or aged mineral dust particles mainly included "reacted $CaCO_3$/$CaMg(CO_3)_2$" and "aluminosilicate + (N, S)", in which (N, S) notation represents compounds containing either nitrates, sulfates, or both. They were produced when aluminosilicate (especially Ca^{2+}-containing) and $CaCO_3$/$CaMg(CO_3)_2$ particles reacted with airborne sulfur and nitrogen oxides in the presence of moisture, or with "secondary acids" such as H_2SO_4, HNO_3, and HCl (Hwang and Ro, 2006; Sullivan et al., 2007). They can also form from adsorption of NH_4NO_3 or $(NH_4)_2SO_4$/NH_4HSO_4 on particle surfaces (Sullivan et al., 2007).

ACPD
10, 26641–26676, 2010

Similarly as with the reacted sea-salt aerosols, the reacted mineral dust particles were classified into three types. The first was nitrate-containing species, including $Ca(NO_3)_2$, such as particles #1, #9, #10, #12, #20, and #103, and "AlSi + (N)," such as particles #13, #15, #17, #23, #41, #102, and #104, in Fig. 3. The second was sulfate-containing species, which include $CaSO_4$ such as particles #31, #35, #70, #75, #78, and #92 and "AlSi + (S)," such as particles #31 and #90, in Fig. 3. The third was both nitrate- and sulfate-containing species, which include $Ca(NO_3)_2$ and $CaSO_4$, such as particles #28 and #48, and "AlSi + (N, S)," such as #4, #45, and #52, in Fig. 3. Results showed that both for Ca- and aluminosilicate-containing particles, nitrate-containing particles were observed more frequently than sulfate- and sulfate- and nitrate-containing ones.

3.1.5 K-containing and Fe-rich particles

K-containing particles are considered to mostly originate from biomass burning. They can also be formed by the reaction of H_2SO_4 with KCl or mineral K_2CO_3 in the air (Ro et al., 2005). Among them, e.g., particles #24, #36, #77, #88, and #99 in Fig. 3, K_2SO_4-containing species are the most abundant. Recent studies have reported that K-containing particles have various sources in the urban environment. For example, large amounts of water-soluble potassium (K^+) can result from meat cooking, refuse incinerators, and, in particular, the use of coal (Wang et al., 2007).

Fe-rich particles look bright on their SEIs (e.g. particles #3 and #7 in Fig. 3). They usually contain more than 20 at.% of Fe, generally in the form of iron ((oxy)hydr)oxides, often with minor amounts of C, Si, and Al. They are often interpreted as goethite, hematite, or magnetite in atmospheric aerosols. Human activities such as mining, steel production, and metallurgical industries, as well as the abrasion of brake lining and erosion of asphalted road, can lead to distinctly higher loads of Fe/FeO_x in urban aerosols (Flament et al., 2008; Kim et al., 2009). The extensive subway system running through the Seoul-Incheon metropolis area, as well as street dust, may also contribute to the emission of Fe-containing particles (Kang et al., 2008).

ACPD
10, 26641–26676, 2010

3.1.6 Fly ash particles

Fly ash is a powdery material made up of tiny glass spheres and composed of mostly silicon, aluminum, iron, and/or calcium oxides. Fly ash particles, largely generated by coal combustion in power plants, can travel long distances through the air, and adsorb organic compounds on their surface (Kim et al., 2008b). They can be easily discerned because they appear in a unique spherical shape (due to high-temperature combustion), and elements of Al, Si, and O are dominant in its chemical compositions, e.g., particles #76, #85, and #97 in Fig. 3. They are quite different from tar balls in composition, although the two types of particles have similar morphologies in secondary electron images.

3.2 Relative abundances of various types of particles

Figure 6 shows the major particle types' relative abundances, obtained by dividing the number of a specific type of particles by the total number of particles analyzed for a sample. In $PM_{2.5-10}$ fractions, reacted sea-salt and reacted mineral dust particles are most frequently encountered, with average relative abundances of 71.1% and 65.0% on haze and non-haze days, respectively; although the abundance of OC particles on haze days is not large, it significantly outnumbers the amount found on non-haze days (on average, 9.8% vs. 3.0%). In the $PM_{1.0-2.5}$ fractions, reacted sea-salt and reacted mineral dust particles on non-haze days significantly outnumber those on haze days (on average, 57.7% vs. 17.5%), while OC particles on haze days significantly outnumber those on non-haze days (on average, 58.7% vs. 13.1%) (Table 2). This means that on haze days, OC particles (especially in $PM_{1.0-2.5}$ fractions) were markedly increased in number, whereas sea-salt and mineral dust particles were decreased. The level of $(NH_4)_2SO_4/NH_4HSO_4$-containing particles also increased on haze days (on average, 1.4% vs. 0.5% for $PM_{2.5-10}$ fractions and 5.5% vs. 2.4% for $PM_{1.0-2.5}$ fractions). Fly ash, K-containing, and Fe-rich particles showed higher abundances on non-haze days than on haze days, both in the $PM_{2.5-10}$ and $PM_{1.0-2.5}$ fractions.

ACPD
10, 26641–26676, 2010

For reacted sea-salt and reacted mineral dust particles in $PM_{2.5-10}$ fractions, nitrate-containing particles significantly outnumbered sulfate-containing and both-containing particles, regardless of whether they were collected on haze or non-haze days (see Fig. 7), suggesting that NO_x in the atmosphere in Incheon had more influence on larger ambient aerosols (aerodynamic diameter ≥2.5 µm) than SO_2. These larger aerosol particles likely originated from the local area, as mass concentrations of local airborne NO_x were greater than those of local SO_2, especially on haze days (see Fig. 8). Also, mass concentrations of airborne PM_{10} on haze days are found to be larger than those on non-haze days. However, for reacted sea-salt and reacted mineral dust particles in $PM_{1.0-2.5}$ fractions, the nitrate-containing particles significantly outnumbered sulfate-containing and both-containing ones on non-haze days, whereas on haze days, sulfate-containing particles were the most abundant (greatly outnumbered the nitrate-containing ones), implying that there were different sources or formation mechanisms for the reacted fine aerosol particles (aerodynamic diameter <2.5 µm) in haze, as compared to non-haze, days. Possible reasons are: on the one hand, SO_2 concentrations on haze days were higher than those on non-haze days (Fig. 8), providing more opportunity for reaction for the fine sea-salt and mineral dust. On the other hand, haze transported from China to Korea via the Yellow Sea or East China Sea was possible (see the transport routes of air masses in Fig. 2). Much of China's haze results from coal burning in industry, power plants, and households, emissions from which contain high sulfur content (Ansmann et al., 2005).

3.3 Possible reasons for elevated OC particles on haze days

Urban areas generally undergo high pollution loads, from sources including heavy traffic, emissions from industrial plants, and intensive energy consumption, which leads to complicated compositions of atmospheric particles. Incheon, one of the largest seaports and cities in Korea, has been facing air pollution problems with its steady increase of fossil fuel consumption. The number of days of low visibility (≤10 km) has significantly increased due to the frequent occurrence of fog, mist, and haze, which is

ACPD
10, 26641–26676, 2010

related to the elevated anthropogenic air pollution and water vapor in the study area (Chung et al., 1999).

As stated above, organic carbon and $(NH_4)_2SO_4/NH_4HSO_4$-containing particles are abundant in haze samples, especially in $PM_{1.0-2.5}$ fractions. A similar observation has been reported for a haze episode that occurred in Guangzhou, China, where airborne $(NH_4)_2SO_4$ and organic compounds were dominant contributors to the $PM_{2.5}$ mass budget (Jung et al., 2009). Herein, possible explanations for the significant increase of OC and $(NH_4)_2SO_4/NH_4HSO_4$-containing particles during the haze episode and their origins are suggested as follows:

- Meteorological factors such as weak winds, high RH and temperature, and "fumigation" along the coast play important roles in the formation of secondary aerosol particles and haze (Soleiman et al., 2003). As Incheon is located near the Yellow Sea, haze formation over Incheon is favored. Wind speeds were slower and RHs were higher (RH=67%–92%) on haze days than on non-haze days, as shown in Table 1. Under stagnant meteorological conditions of slow wind speed and high RH, ultrafine particles converted from gaseous species could remain for a longer time, and hygroscopic particles could grow to become larger ones, with aerodynamic diameters of >0.1 µm (Carrico et al., 2010), which favors haze formation with elevated aerosol levels. Studies have reported that, based on the investigation of chemical characteristics of acidic gas pollutants and $PM_{2.5}$ during hazy episodes in Seoul, Korea, the fine aerosols responsible for haze formation are mostly secondary OC particles produced by photochemical smog or photochemical reactions (Kang et al., 2004; Noh et al., 2009).

- Although chemical analysis has shown that the major aerosol constituents in haze phenomena at Syowa Station, Antarctica, were sea-salts (e.g., Na^+, Cl^-) (Hara, et al., 2010), abundant sea-salt particles, genuine or reacted, were not encountered in the Incheon haze samples (although Incheon is located near the Yellow sea). It is suggested that haze formation in Incheon has a unique mechanism

ACPD
10, 26641–26676, 2010

(not owing to the increase of sea-salt aerosols). The most likely source of $PM_{2.5}$ and OC particles is from automotive vehicles, which have been sharply increasing in number due to rapid urbanization and motorization (Timilsina and Shrestha, 2009). Since Incheon is one of the largest cities in Korea, densely populated with about 700 000 motor vehicles, and motor vehicle exhaust accounted for >80% of air pollution in the area (Kim et al., 2006), it is suggested that much of the organic aerosol burden in Incheon can be attributed to automotive vehicle sources. For example, a number of freight vehicles, i.e., heavy-duty trucks (diesel vehicles), travel along the highway carrying goods to the wharves at Incheon seaport; most of the short-term transients for commuting are attributable to local traffic sources. The higher OC and EC levels are often observed during the morning traffic hours (Kim et al., 2006). In addition, automobile vehicles are an important source of NO_x and $PM_{2.5}$ emissions (Dallmann and Harley, 2010), so the high mass concentration of atmospheric NO_x in Incheon (shown in Fig. 8) likely results from motor vehicles. It is certain that air pollutants emitted from motor vehicles are a significant factor in haze formation in Incheon.

The higher abundance of $(NH_4)_2SO_4/NH_4HSO_4$-containing particles on haze days is likely because the gas-to-particle conversion of SO_2 to sulfate and the reactions of H_2SO_4/sulfate are accelerated during haze days under stagnation conditions (Tan et al., 2009). Atmospheric SO_2 could be due to industrial emissions (such as coal-fired power plants and steel factories) in Incheon and China.

– Biomass burning events can greatly degrade the local air quality, and under stagnant atmospheric conditions can also cause long-lasting regional haze phenomena (Ryu et al., 2007). Some haze phenomena have been reported to be associated with outflow of biomass burning (one of the major sources of fine carbonaceous aerosols to the atmosphere) (Hara et al., 2010; Hoffer et al., 2006). It is likely that biomass burning at the rural areas around Incheon is responsible for the increase of OC particles on haze days (Kim et al., 2006; Park et al., 2006). In Korea, open-field burning of agricultural wastes after harvest has been a common

ACPD
10, 26641–26676, 2010

practice. One typical seasonal biomass burning period occurs in the spring, when agricultural wastes are burned after the harvesting of barley, and the other in the fall (around October) after the harvesting of rice (Ryu et al., 2004). Elevated levels of $PM_{2.5}$ and organic carbons have been observed during agricultural waste burning episodes in October (Ryu et al., 2004, 2007; Bi et al., 2008), suggesting the influence of agricultural burning on ambient fine particulate matters, especially of organic species. In addition, barbecue parties are popularly held during autumn events in Korea, where a significant amount of OC aerosols can also be emitted (Ryu et al., 2004).

Many studies have reported that relatively high levels of water-soluble potassium (K^+) is present in biomass burning plumes, and therefore potassium has been widely used as a tracer of biomass burning in source-apportionment studies (Wang et al., 2007; Andreae, 1983). However, in the present study, no significant difference in abundance of K-containing particles between samples from haze and non-haze days was observed (Table 2), implying that biomass burning was not a major contributor to this haze episode.

– Regional haze episodes frequently occur in northern and eastern China, from which aerosol particles can be transported over a long distance, for example, from East China to the Korean peninsula (Sun et al., 2006). Hence, the Korean peninsula has often been affected by long-range transported aerosols such as Asian dust, forest-fire smoke, and anthropogenic aerosols under westerly wind conditions (Ryu et al., 2004). For example, on 17, 24, and 25 October 2005, severe haze had lingered over Eastern China, which finally headed toward the Yellow Sea and Korea, resulting in elevated OC and EC levels in Gwangju (Noh et al., 2004; Hong et al., 2008; Lee et al., 2006). Some of the images acquired from the Moderate Resolution Imaging Spectroradiometer (MODIS) on NASA's Terra satellite (e.g. the MODIS images on 2 and 28 October 2009 from the website: http://spacegizmo.livingdazed.com/tag/china-haze) also demonstrated that haze can be transported from China to Korea via the Yellow Sea or East China Sea.

ACPD
10, 26641–26676, 2010

4 Conclusions

Twelve sets of aerosol particle samples were collected on Al foils by using a three-stage cascade impactor (the aerodynamic cut-off diameters for stages 1–3 are >10, 2.5–10, and 1.0–2.5 µm, respectively) in Incheon, Korea on 13–18 October 2008, during which a typical haze episode occurred (on 15–18 October). Using low-*Z* particle EPMA, a quantitative ED-EPMA technique, 3600 ambient aerosol particles overall, ranging 2.5–10 µm (stage 2) and 1.0–2.5 µm (stage 3) in aerodynamic diameter, were measured, and the morphology and chemical composition of every particle were analyzed. For identified particle types such as carbonaceous, $(NH_4)_2SO_4/NH_4HSO_4$-containing, sea-salt, mineral dust, K-containing, Fe-rich, and fly ash particles, organic carbon (OC) and $(NH_4)_2SO_4/NH_4HSO_4$-containing particles were more abundant in $PM_{1.0-2.5}$ fractions than in $PM_{2.5-10}$ fractions, and were greatly increased on haze days compared with those on non-haze days. During the haze period, relative abundances of OC and $(NH_4)_2SO_4/NH_4HSO_4$particles were increased in $PM_{2.5-10}$ fractions 2.7- and 2.8-fold, respectively, and increased in $PM_{1.0-2.5}$ fractions 3.5- and 1.3-fold, respectively. Furthermore, in $PM_{1.0-2.5}$ fractions, the nitrate-containing reacted particles (sea-salt and mineral dust particles reacting with airborne NO_x/HNO_3) significantly outnumbered the sulfate-containing ones (sea-salt and mineral dust particles reacting with airborne SO_2/H_2SO_4) on non-haze days while the reverse was true on haze days, which was indicative of special sources or formation mechanisms for reacted fine aerosol particles (aerodynamic diameter <2.5 µm) in the process of haze formation. Results indicated that motor vehicles, the burning of biomass in the areas surrounding Incheon, and haze from Eastern China were the major contributors to urban haze formation in Incheon.

Acknowledgements. This work was supported by the Korean Science and Engineering Foundation (KOSEF) grant funded by the Korea government (MOST) (ROA-2007-000-20030-0).

ACPD
10, 26641–26676, 2010

References

Adachi, K. and Buseck, P. R.: Internally mixed soot, sulfates, and organic matter in aerosol particles from Mexico City, Atmos. Chem. Phys., 8, 6469–6481, doi:10.5194/acp-8-6469-2008, 2008.

Adachi, K., Chung, S. H., and Buseck, P. R.: Shapes of soot aerosol particles and implications for their effects on climate, J. Geophys. Res., 115, D15206, doi:10.1029/2009JD012868, 2010.

Aiken, A. C., Salcedo, D., Cubison, M. J., Huffman, J. A., DeCarlo, P. F., Ulbrich, I. M., Docherty, K. S., Sueper, D., Kimmel, J. R., Worsnop, D. R., Trimborn, A., Northway, M., Stone, E. A., Schauer, J. J., Volkamer, R. M., Fortner, E., de Foy, B., Wang, J., Laskin, A., Shutthanandan, V., Zheng, J., Zhang, R., Gaffney, J., Marley, N. A., Paredes-Miranda, G., Arnott, W. P., Molina, L. T., Sosa, G., and Jimenez, J. L.: Mexico City aerosol analysis during MILAGRO using high resolution aerosol mass spectrometry at the urban supersite (T0) – Part 1: Fine particle composition and organic source apportionment, Atmos. Chem. Phys., 9, 6633–6653, doi:10.5194/acp-9-6633-2009, 2009.

Andreae, M. O.: Soot carbon and excess fine potassium: long-range transport of combustion-derived aerosols, Science, 220, 1148–1151, 1983.

Ansmann, A., Engelmann, R., Althausen, D., Wandinger, U., Hu, M., Zhang, Y., and He, Q.: High aerosol load over the Pearl River Delta, China, observed with Raman lidar and Sun photometer, Geophys. Res. Lett., 32, L13815, doi:10.1029/2005GL023094, 2005.

Arimoto, R., Kim, Y. J., Kim, Y. P., Quinn, P. K., Bates, T. S., Anderson, T. L., Gong, S., Uno, I., Chin, M., Huebert, B. J., Clarke, A. D., Shinozuka, Y., Weber, R. J., Anderson, J. R., Guazzotti, S. A., Sullivan, R. C., Sodeman, D. A., Prather, K. A., and Sokolik, I. N.: Characterization of Asian Dust during ACE-Asia, Global Planet Change, 52, 23–56, 2006.

Athanasopoulou, E., Tombrou, M., Pandis, S. N., and Russell, A. G.: The role of sea-salt emissions and heterogeneous chemistry in the air quality of polluted coastal areas, Atmos. Chem. Phys., 8, 5755–5769, doi:10.5194/acp-8-5755-2008, 2008.

Bi, X., Simoneit, B. R. T., Sheng, G., Ma, S., and Fu, J.: Composition and major sources of organic compounds in urban aerosols, Atmos. Res., 88, 256–265, 2008.

Brown, S. G., Herckes, P., Ashbaugh, L., Hannigan, M. P., Kreidenweis, S. M., and Collett Jr., J. L.: Characterization of organic aerosol in Big Bend National Park, Texas, Atmos. Environ., 36, 5807–5818, 2002.

ACPD
10, 26641–26676, 2010

Carrico, C. M., Petters, M. D., Kreidenweis, S. M., Sullivan, A. P., McMeeking, G. R., Levin, E. J. T., Engling, G., Malm, W. C., and Collett Jr., J. L.: Water uptake and chemical composition of fresh aerosols generated in open burning of biomass, Atmos. Chem. Phys., 10, 5165–5178, doi:10.5194/acp-10-5165-2010, 2010.

Chakrabarty, R. K., Moosmüller, H., Chen, L.-W. A., Lewis, K., Arnott, W. P., Mazzoleni, C., Dubey, M. K., Wold, C. E., Hao, W. M., and Kreidenweis, S. M.: Brown carbon in tar balls from smoldering biomass combustion, Atmos. Chem. Phys., 10, 6363–6370, doi:10.5194/acp-10-6363-2010, 2010.

Choel, M., Deboudt, K., Osan, J., Flament, P., and van Grieken, R.: Quantitative determination of low-Z elements in single atmospheric particles on boron substrates by automated scanning electron microscopy-energy-dispersive X-ray spectrometry, Anal. Chem., 77, 5686–5692, 2005.

Chun, Y. and Lim, J. Y.: The recent characteristics of Asian dust and haze events in Seoul, Korea, Meteorol. Atmos. Phys., 87, 143–152, 2004.

Chung, Y. S., Kim, H. S., and Yoon, M. B.: Observations of visibility and chemical compositions related to fog, mist and haze in South Korea, Water Air Soil Poll., 111, 139–157, 1999.

Dallmann, T. R. and Harley, R. A.: Evaluation of mobile source emission trends in the United States, J. Geophys. Res., 115, D14305, doi:10.1029/2010JD013862, 2010.

Davis, M. E., Laden, F., Hart, J. E., Garshick, E., and Smith, T. J.: Economic activity and trends in ambient air pollution, Environ. Health Perspect., 118, 614–619, 2010.

Feng, Y., Chen, Y., Guo, H., Zhi, G., Xiong, S., Li, J., Sheng, G., and Fu, J.: Characteristics of organic and elemental carbon in $PM_{2.5}$ samples in Shanghai, China, Atmos. Res., 92, 434–442, 2009.

Flament, P., Mattielli, N., Aimoz, L., Choël, M., Deboudt, K., de Jong, J., Rimetz-Planchon, J., and Weis, D.: Iron isotopic fractionation in industrial emissions and urban aerosols, Chemosphere, 73, 1793–1798, 2008.

Geng, H., Ryu, J., Jung, H.-J., Chung, H., Ahn, K. H., and Ro, C.-U.: Single-particle characterization of summertime arctic aerosols collected at Ny-Alesund, Svalbard, Environ. Sci. Technol., 44, 2348–2353, 2010.

Geng, H., Jung, H.-J., Park, Y., Hwang, H., Kim, H., Kim, Y. J., Sunwoo, Y., and Ro, C.-U.: Morphological and chemical composition characteristics of summertime atmospheric particles collected at Tokchok Island, Korea, Atmos. Environ., 43, 3364–3373, 2009a.

Geng, H., Park, Y., Hwang, H., Kang, S., and Ro, C.-U.: Elevated nitrogen-containing particles

ACPD
10, 26641–26676, 2010

observed in Asian dust aerosol samples collected at the marine boundary layer of the Bohai Sea and the Yellow Sea, Atmos. Chem. Phys., 9, 6933–6947, doi:10.5194/acp-9-6933-2009, 2009b.

Hara, K., Osada, K., Yabuki, M., Hashida, G., Yamanouchi, T., Hayashi, M., Shiobara, M., Nishita, C., and Wada, M.: Haze episodes at Syowa Station, coastal Antarctica: Where did they come from?, J. Geophys. Res., 115, D14205, doi:10.1029/2009JD012582, 2010.

Hoffer, A., Gelencsér, A., Blazsó, M., Guyon, P., Artaxo, P., and Andreae, M. O.: Diel and seasonal variations in the chemical composition of biomass burning aerosol, Atmos. Chem. Phys., 6, 3505–3515, doi:10.5194/acp-6-3505-2006, 2006.

Hoffman, R. C., Laskin A., and Finlayson-Pitts, B. J.: Sodium nitrate particles: physical and chemical properties during hydration and dehydration, and implications for aged sea salt aerosols, J. Aerosol Sci., 35, 869–887, 2004.

Hong, S. B., Kim, D. S., Ryu, S. Y., Kim, Y. J., and Lee, J. H.: Chemical characteristics of $PM_{2.5}$ ions measured by a semicontinuous measurement system during the fall season at a suburban site, Gwangju, Korea, Atmos. Res., 89, 62–75, 2008.

Hwang, H. J. and Ro, C.-U.: Direct observation of nitrate and sulfate formations from mineral dust and sea-salts using low-*Z* particle electron probe X-ray microanalysis, Atmos. Environ., 40, 3869–3880, 2006.

Jacobson, M. Z.: Strong radiative heating due to the mixing state of black carbon in atmospheric aerosols, Nature, 409, 695–697, 2001.

Johnson, K. S., Zuberi, B., Molina, L. T., Molina, M. J., Iedema, M. J., Cowin, J. P., Gaspar, D. J., Wang, C., and Laskin, A.: Processing of soot in an urban environment: case study from the Mexico City Metropolitan Area, Atmos. Chem. Phys., 5, 3033–3043, doi:10.5194/acp-5-3033-2005, 2005.

Jung, H.-J., Malek, M. A., Ryu, J., Kim, B., Song, Y.-C., Kim, H., and Ro, C.-U.: Speciation of individual mineral particles of micrometer size by the combined use of attenuated total reflectance-fourier transform-infrared imaging and quantitative energy-dispersive electron probe X-ray microanalysis techniques, Anal. Chem, 82, 6193–6202, 2010.

Jung, J., Lee, H., Kim, Y. J., Liu, X., Zhang, Y., Gu, J., and Fan, S.: Aerosol chemistry and the effect of aerosol water content on visibility impairment and radiative forcing in Guangzhou during the 2006 Pearl River Delta campaign, J. Environ. Manage., 90, 3231–3244, 2009.

Kang, C. M., Lee, H. S., Kang, B. W., Lee, S. K., and Sunwoo, Y.: Chemical characteristics of acidic gas pollutants and $PM_{2.5}$ species during hazy episodes in Seoul, South Korea, Atmos.

ACPD
10, 26641–26676, 2010

Environ., 38, 4749–4760, 2004.
Kang, S., Hwang, H., Park, Y., Kim, H., and Ro, C.-U.: Chemical compositions of subway particles in Seoul, Korea determined by a quantitative single particle analysis, Environ. Sci. Technol., 42, 9051–9057, 2008.
Keywood, M. D., Ayers, G. P., Gras, J. L., Boers, R., and Leong, C. P.: Haze in the Klang Valley of Malaysia, Atmos. Chem. Phys., 3, 591–605, doi:10.5194/acp-3-591-2003, 2003.
Kim, Y. J., Kim, M. J., Lee, K. H., and Park, S. S.: Investigation of carbon pollution episodes using semi-continuous instrument in Incheon, Korea, Atmos. Environ., 40, 4064–4075, 2006.
Kim, K. W., Kim, Y. J., and Bang, S. Y.: Summer time haze characteristics of the urban atmosphere of Gwangju and the rural atmosphere of Anmyon, Korea, Environ. Monit. Assess., 141, 189–199, 2008a.
Kim, W., Doh, S.-J., and Yu, Y.: Anthropogenic contribution of magnetic particulates in urban roadside dust, Atmos. Environ., 43, 3137–3144, 2009.
Kim, W., Doh, S.-J., Yu, Y., and Lee, M.: Role of Chinese wind-blown dust in enhancing environmental pollution in Metropolitan Seoul, Environ. Pollut., 153, 333–341, 2008b.
Laskin, A., Gaspar, D. J., Wang W., Hunt, S. W., Cowin, J. P., Colson, S. D., and Finlayson-Pitts, B. J.: Reactions at interfaces as a source of sulfate formation in sea-salt particles, Science, 301, 340–344, 2003.
Laskin A., Iedema M. J., and Cowin, J. P.: Quantitative time-resolved monitoring of nitrate formation in sea salt particles using a CCSEM/EDX single particle analysis, Environ. Sci. Technol., 36, 4948–4955, 2002.
Lee, K. H., Kim, Y. J., and Kim, M. J.: Characteristics of aerosol observed during two severe haze events over Korea in June and October 2004, Atmos. Environ., 40, 5146–5155, 2006.
Lee, Y. L. and Sequeira, R.: Visibility degradation across Hong Kong: its components and their relative contributions, Atmos. Environ., 34, 5861–5872, 2001.
Li, W. and Bai, Z.: Characteristics of organic and elemental carbon in atmospheric fine particles in Tianjin, China, Particuology, 7, 432–437, 2009.
Menon, S., Hansen, J., Nazarenko, L., and Luo, Y.: Climate effects of black carbon aerosols in China and India, Science, 297, 2250–2253, 2002.
Millstein, D. E., Harley, R. A., and Hering, S. V.: Weekly cycles in fine particulate nitrate, Atmos. Environ., 42, 632–641, 2008.
Moffet, R. C. and Prather K. A.: In-situ measurements of the mixing state and optical properties of soot with implications for radiative forcing estimates, P. Natl. Acad. Sci. USA, 106, 11872–

ACPD
10, 26641–26676, 2010

11877, 2009.
Moffet, R. C., Henn, T. R., Tivanski, A. V., Hopkins, R. J., Desyaterik, Y., Kilcoyne, A. L. D., Tyliszczak, T., Fast, J., Barnard, J., Shutthanandan, V., Cliff, S. S., Perry, K. D., Laskin, A., and Gilles, M. K.: Microscopic characterization of carbonaceous aerosol particle aging in the outflow from Mexico City, Atmos. Chem. Phys., 10, 961–976, doi:10.5194/acp-10-961-2010, 2010.
Noh, Y. M., Müller, D., Shin, D. H., Lee, H., Jung, J. S., Lee, K. H., Cribb, M., Li, Z., and Kim, Y. J.: Optical and microphysical properties of severe haze and smoke aerosol measured by integrated remote sensing techniques in Gwangju, Korea, Atmos. Environ., 43, 879–888, 2009.
Oum, K. W., Lakin, M. J., DeHaan, D. O., Brauers, T., and Finlayson-Pitts, B. J.: Formation of molecular chlorine from the photolysis of ozone and aqueous sea-salt particles, Science, 279, 74–77, 1998.
Park, S. S., Bae, M.-S., Schauer, J. J., Kim, Y. J., Cho, S. Y., and Kim, S. J.: Molecular composition of $PM_{2.5}$ organic aerosol measured at an urban site of Korea during the ACE-Asia campaign, Atmos. Environ., 40, 4182–4198, 2006.
Ro, C.-U., Osan, J., Szaloaki, I., Oh, K. Y., and Van Grieken, R.: Determination of chemical species in individual aerosol particles using ultrathin window EPMA, Environ. Sci. Technol., 34, 3023–3030, 2000.
Ro, C.-U., Oh, K. Y., Kim, H., Kim, Y. P., Lee, S. B., Kim, K. H., Chang, H. K., Osan, J., de Hong, J., Worobiec, A., and Van Grieken, R.: Single-particle analysis of aerosols at Cheju Island, Korea, using low-*Z* electron probe X-ray microanalysis: A direct proof of nitrate formation from sea salts, Environ. Sci. Technol., 35, 4487–4494, 2001.
Ro, C.-U., Osan, J., Szaloki, I., de Hoog, J., Worobiec, A., and Van Grieken, R.: A Monte Carlo program for quantitative electron-induced X-ray analysis of individual particles, Anal. Chem., 75, 851–859, 2003.
Ro, C.-U., Kim, H., and Van Grieken, R.: An expert system for chemical speciation of individual particles using low-*Z* particle electron probe X-ray microanalysis data, Anal. Chem., 76, 1322–1327, 2004.
Ro, C.-U., Hwang, H., Kim, H., Chun, Y., and Van Grieken, R.: Single-particle characterization of four Asian Dust samples collected in Korea, using low-*Z* particle electron probe X-ray microanalysis, Environ. Sci. Technol., 39, 1409–1419, 2005.
Ro, C.-U.: Quantitative energy-dispersive electron probe X-ray microanalysis of individual par-

ACPD
10, 26641–26676, 2010

ticles, Powder Diffr., 21, 140–144, 2006.
Ryu, S. Y., Kim, J. E., Zhuanshi, H., Kim, Y. J., and Kang, G. U.: Chemical composition of post-harvest biomass burning aerosols in Gwangju, Korea, J. Air Waste Manage., 54, 1124–1137, 2004.
Ryu, S. Y., Kwon, B. G., Kim, Y. J., Kim, H. H., and Chun K. J.: Characteristics of biomass burning aerosol and its impact on regional air quality in the summer of 2003 at Gwangju, Korea, Atmos. Res., 84, 362–373, 2007.
Schichtel, B. A., Husar, R. B., Falke, S. R., and Wilson, W. E.: Haze trends over the United States, 1980–1995, Atmos. Environ., 35, 5205–5210, 2001.
Soleiman, A., Othman, M., Samah, A. A., Sulaiman, N. M., and Radojevic, M.: The occurrence of haze in Malaysia: a case study in an urban industrial area, Pure Appl. Geophys., 160, 221–238, 2003.
Sullivan, R. C., Guazzotti, S. A., Sodeman, D. A., Tang, Y., Carmichael, G. R., and Prather, K. A.: Mineral dust is a sink for chlorine in the marine boundary layer, Atmos. Environ., 41, 7166–7179, 2007.
Sun, Y., Zhuang, G., Tang, A. A., Wang, Y., and An, Z.: Chemical Characteristics of $PM_{2.5}$ and PM_{10} in haze-fog episodes in Beijing, Environ. Sci. Technol., 40, 3148–3155, 2006.
Takahama, S., Gilardoni, S., Russell, L. M., and Kilcoyne, A. L. D.: Classification of multiple types of organic carbon composition in atmospheric particles by scanning transmission X-ray microscopy analysis, Atmos. Environ., 41, 9435–9451, 2007.
Tan, J.-H., Duan, J.-C., Chen, D.-H., Wang, X.-H., Guo, S.-J., Bi, X.-H., Sheng, G.-Y., He, K.-B., and Fu, J.-M.: Chemical characteristics of haze during summer and winter in Guangzhou, Atmos. Res., 94, 238–245, 2009.
Timilsina G. R. and Shrestha, A.: Transport sector CO_2 emissions growth in Asia: Underlying factors and policy options, Energ. Policy, 37, 4523–4539, 2009.
Vekemans, B., Janssens, K., Vincze, L., Adams, F., and Van Espen, P.: Analysis of X-ray spectra by iterative least squares (AXIL): new developments, X-Ray Spectrom., 23, 278–285, 1994.
Viezee, W. and Oblanas, J.: Lidar-observed haze layers associated with thermal structure in the lower atmosphere, J. Appl. Meteor., 8, 369–375, 1969.
Wang, Q., Shao, M., Liu, Y., William, K., Paul, G., Li, X., Liu, Y., and Lu, S.: Impact of biomass burning on urban air quality estimated by organic tracers: Guangzhou and Beijing as cases, Atmos. Environ., 41, 8380–8390, 2007.

ACPD
10, 26641–26676, 2010

Watson, J. G.: Visibility: Science and regulation, J. Air Waste Manage., 52, 628–713, 2002.
Yadav, A. K., Kumar, K., Kasim, A., Sing, M. P., Parida, S. K., and Sharan, M.: Visibility and incidence of respiratory diseases during the 1998 haze episode in Brunei Darussala, J. Air Waste Manage., 53, 946–956, 2003.

ACPD
10, 26641–26676, 2010

Table 1. Sampling times and meteorological conditions and PM_{10} concentrations during samplings.

No.	sampling date	Local time (KST)	Temperature during sampling (°C)	RH during sampling (%)	Wind speed (m/s)
1	a.m. 13 Oct, 2008	10:15~11:45	17.9	56	2.0
2	p.m. 13 Oct, 2008	19:00~20:11	16.8	68	1.9
3	a.m. 14 Oct, 2008	10:05~11:50	19.3	58	2.1
4	p.m. 14 Oct, 2008	19:03~20:00	17.7	69	1.8
5	a.m. 15 Oct, 2008	10:10~11:30	19.4	73	1.5
6	p.m. 15 Oct, 2008	18:55~20:30	18.1	81	1.1
7	a.m. 16 Oct, 2008	10:10~11:00	19.8	67	0.8
8	p.m. 16 Oct, 2008	19:12~20:34	18.6	92	1.2
9	a.m. 17 Oct, 2008	10:10~11:30	18.9	79	2.0
10	p.m. 17 Oct, 2008	19:30~21:05	18.7	90	1.4
11	a.m. 18 Oct, 2008	10:06~10:50	20.1	68	0.7
12	p.m. 18 Oct, 2008	19:40~20:45	20.0	75	1.0

ACPD
10, 26641–26676, 2010

Table 2. Relative abundances of particle types on haze vs. non-haze days.

Particle types	Relative abundances in $PM_{2.5-10}$ fraction (%)		Relative abundances in $PM_{1.0-2.5}$ fraction (%)	
	non-haze days	haze days	non-haze days	haze days
1. genuine mineral dust	10.3±3.4	12.7±5.4	9.3±5.0	5.8±5.5
2. reacted mineral dust	46.0±2.7	49.5±9.2	29.7±11.2*	10.6±8.6
3. genuine sea-salt	1.1±1.6	0.5±0.9	0.8±1.1	0.6±1.1
4. reacted sea-salt (& mixtures)	25.1±6.9	15.5±9.6	28.0±8.5**	6.9±3.7
5. EC (elemental carbon)	2.8±2.1	3.2±2.1	5.9±4.4	5.1±3.1
6. OC (organic carbon)	3.0±2.2*	9.8±4.9	13.1±7.0**	58.7±19.8
7. $(NH_4)_2SO_4/NH_4HSO_4$-containing	0.5±0.7	1.4±1.8	2.4±1.7	5.5±4.3
8. fly ash	3.8±2.8	2.5±1.7	4.3±2.6	1.2±1.5
9. K-containing	2.0±1.5	1.9±3.1	4.2±4.3	3.8±2.3
10. Fe-rich	5.4±1.5*	3.0±1.5	2.3±1.9	1.9±2.8

Note:

(1) The non-haze samples were collected on 13 and 14 October 2008 and in the morning of 15 October 2008; the haze samples were collected in the afternoon of 15 October 2008 and on 16–18 October 2008.

(2) The student t-test was used to compare the difference of relative abundances for different particle types between haze and non-haze days. The difference was regarded as significant when $^{*}P \leq 0.05$; $^{**}P \leq 0.01$.

(3) The data are expressed as "mean ± S.D.".

ACPD
10, 26641–26676, 2010

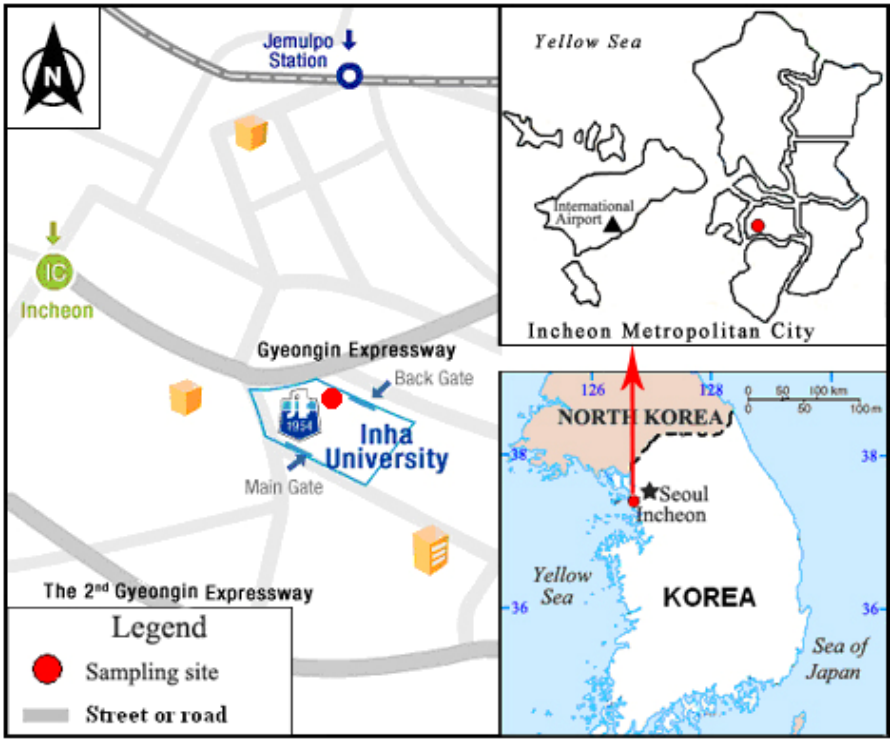

Fig. 1. A schematic map of the sampling site.

ACPD
10, 26641–26676, 2010

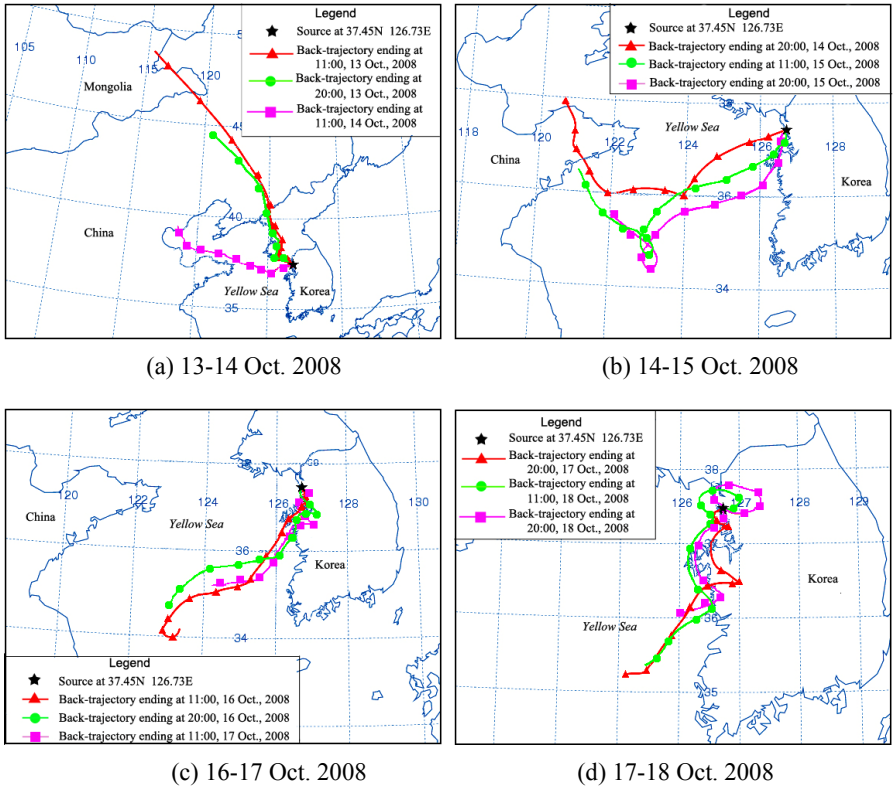

(a) 13-14 Oct. 2008

(b) 14-15 Oct. 2008

(c) 16-17 Oct. 2008

(d) 17-18 Oct. 2008

Fig. 2. 72-h backward air-mass trajectories at sampling height (around 40 m above sea level) from 13 to 18 October 2008 (KST).

ACPD
10, 26641–26676, 2010

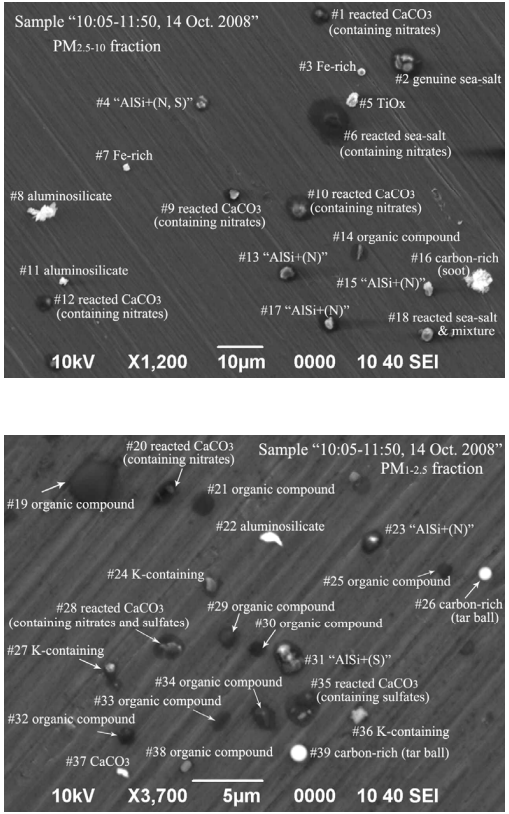

(a) Sample 3, collected at "10:05-11:50, 14 Oct. 2008"
(upper: $PM_{10\text{-}2.5}$ fraction; down: $PM_{1.0\text{-}2.5}$ fraction)

Fig. 3. Typical SEM images of urban aerosol particles collected in Incheon, Korea (for convenience, aluminosilicate is denoted as "AlSi-containing". "(N)" notation represents particles containing nitrates; "(S)" notation represents particles containing sulfates; "(N, S)" notation represents particles containing both nitrates and sulfates. (C, N, O, S) notation represents the mixture of carbonaceous and $(NH_4)_2SO_4/NH_4HSO_4$ particles).

ACPD
10, 26641–26676, 2010

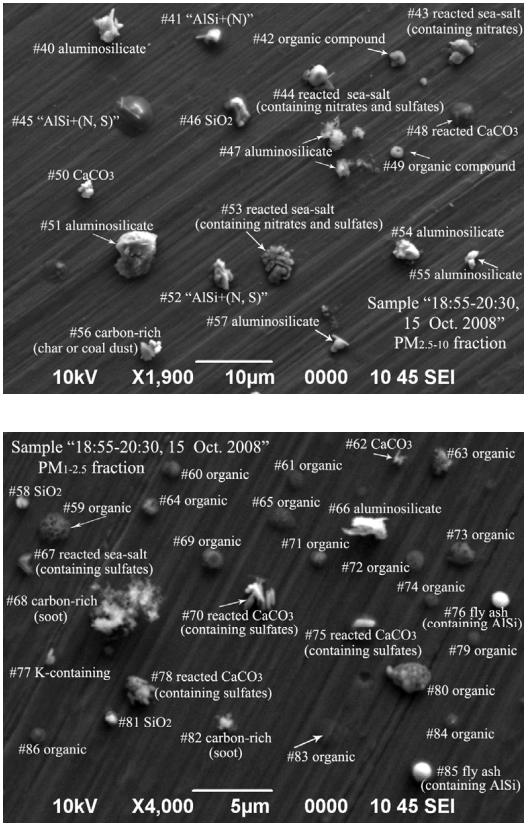

(b) Sample 6, collected at "18:55-20:30, 15 Oct. 2008" (upper: $PM_{10\text{-}2.5}$ fraction; down: $PM_{1.0\text{-}2.5}$ fraction)

Fig. 3. Continued.

ACPD
10, 26641–26676, 2010

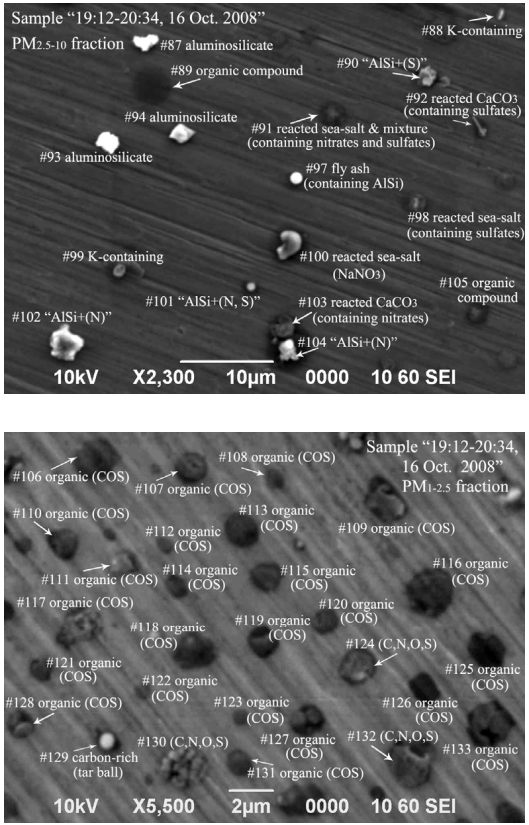

(c) Sample 8, collected at "19:12-20:34, 16 Oct. 2008"

(upper: $PM_{10\text{-}2.5}$ fraction; down: $PM_{1.0\text{-}2.5}$ fraction)

Fig. 3. Continued.

ACPD
10, 26641–26676, 2010

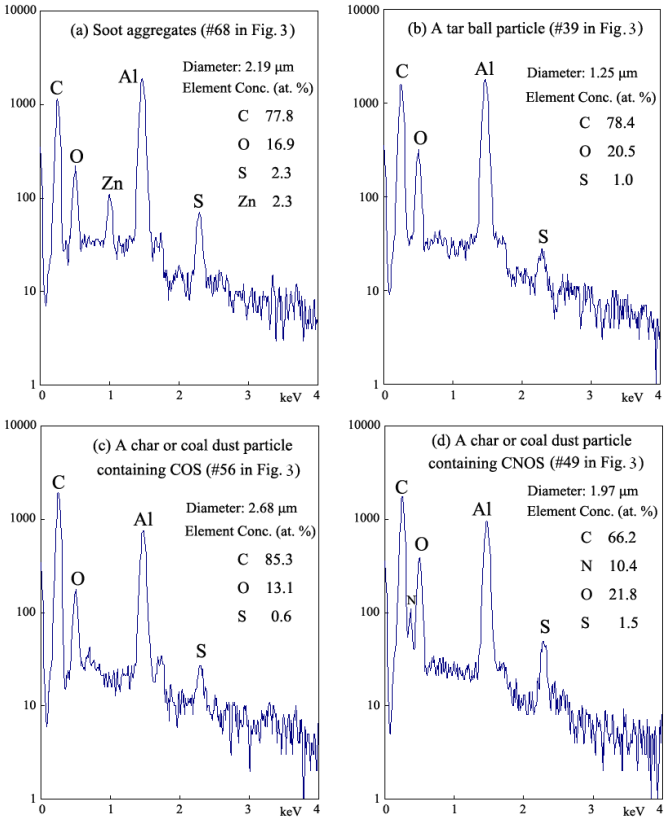

Fig. 4. X-ray spectra and atomic concentrations of carbon-rich particles (Al X-ray peaks are from collecting substrates).

ACPD
10, 26641–26676, 2010

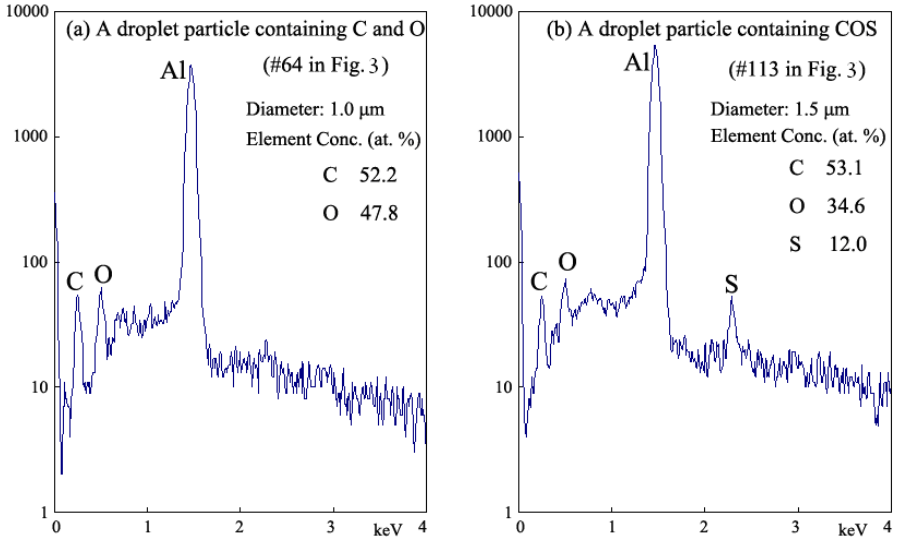

Fig. 5. X-ray spectra and atomic concentrations of organic carbon (OC) particles (Al X-ray peaks are from collecting substrates).

ACPD
10, 26641–26676, 2010

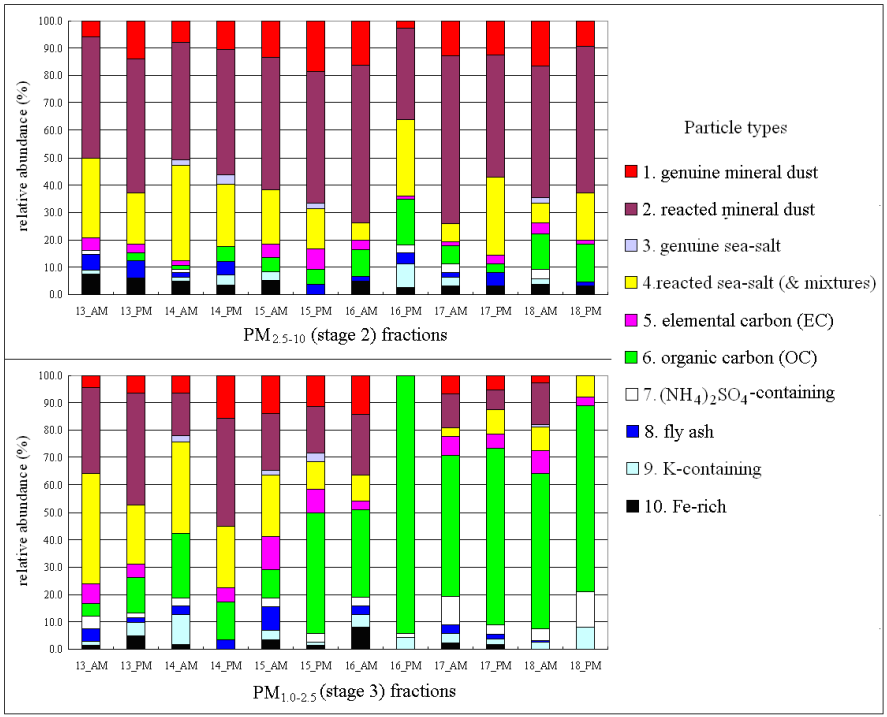

Fig. 6. Relative abundances of different particle types for the 12 sets of samples.

ACPD
10, 26641–26676, 2010

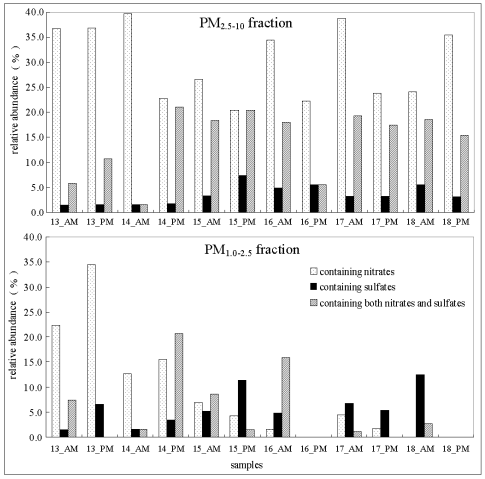

(a) reacted (aged) mineral dust particles

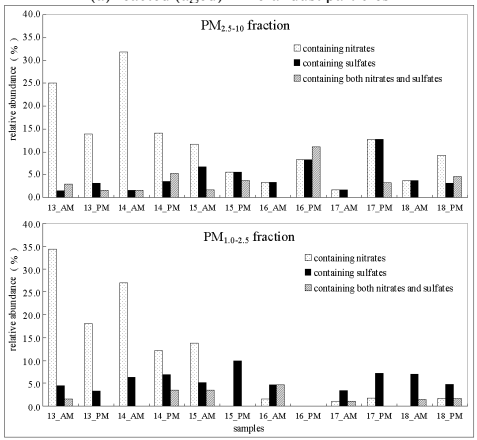

(b) reacted (aged) sea-salt (& mixture) particles

Fig. 7. Relative abundances of reacted mineral dust and reacted sea-salt particles containing nitrates, sulfates, and both.

ACPD
10, 26641–26676, 2010

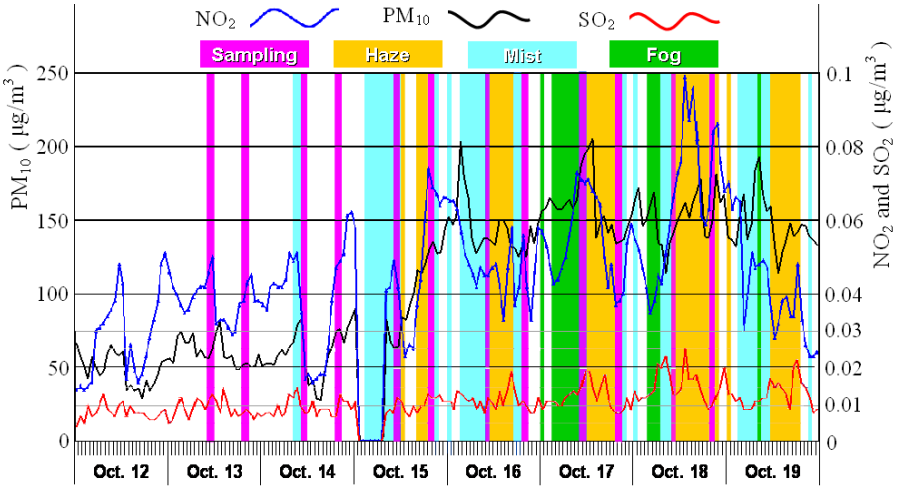

Fig. 8. Mass concentrations (μg/m^3) of air pollutants (PM_{10}, SO_2, and NO_2) on haze and non-haze days.

ACPD
10, 26641–26676, 2010